Residual chlorine prevents full densification of flash sintered yttria-stabilized zirconia ceramics

Vladimír Prajzler [a, b, *], Karel Maca [a], Richard Todd [b]

[a] Brno University of Technology, CEITEC, Purkyňova 123, 612 00 Brno, Czech Republic

[b] University of Oxford, Department of Materials, Parks Road, Oxford OX1 3PH, United Kingdom

[*] Corresponding author at: Brno University of Technology, CEITEC, Purkyňova 123, 612 00 Brno, Czech Republic. E-mail address: vladimir.prajzler@ceitec.vutbr.cz

Abstract

The densification of yttria-stabilized zirconia (YSZ) during flash sintering is strongly dependent on the amount of residual chlorine in the sintered bodies. The residual chlorine, present as a remnant from powder synthesis, hinders densification after it is trapped and vaporized in the rapidly closing pores, limiting the final density at around 87 – 93 % of theoretical. We show that this phenomenon is likely to affect all YSZ powders synthesized from chloride precursors unless the residual chlorine is reduced to ≤ 0.03 wt% before the onset of the flash sintering. This can be universally achieved by thermal purification of green bodies at a high temperature or by chemical purification in ammonium hydroxide. Furthermore, added binder in commercially available Tosoh zirconia TZ-powders (TZ-3YB, TZ-3YB-E) helps to significantly reduce chlorine content during binder burnout which in turn allows flash sintering into a high density even without green body purification.

Key words

Flash sintering, Zirconia, Densification, Shell-like structure

1. Introduction

The flash sintering technique utilizes enormously high heating rates (up to ~ 10^4 °C/min) which significantly accelerates densification of ceramic materials [1–3]. The densification of flash sintered yttria-stabilized zirconia (YSZ) ceramics usually takes place in the order of seconds, making the shrinkage and pore closure extremely fast compared to conventional sintering. A high heating rate also limits the extent of non-densifying surface diffusion, and thus, pore coalescence [4,5]. This essentially means that none of the pores are growing during densification which is an excellent condition for achieving full density and fine-grained microstructure.

Although the current state of the flash sintering technology faces many processing issues which must be resolved before wider industrial application, many studies suggest that the flash sintering of YSZ powders can lead to a nearly/fully dense compact [6–18]. This is a desirable outcome, however, several studies reported limited densification despite of employing a relatively high current density and a long dwell time in the flash state [19–25]. Moreover, poorly densified YSZ specimens with densities lower than 90 % of theoretical density (TD) are also no exception in the relevant literature [10,11,15,26]. These apparently conflicting reports, where some of the YSZ powders can be fully sintered and some not, closely resemble the behaviour observed in fast-fired YSZ ceramics [27–31].

In fast firing, the green body is pushed into the preheated furnace which results in a high heating rate as well, usually in between 10^2-10^3 °C/min [32,33], and the specimen is mainly heated by a thermal radiation coming from the heating elements [34,35]. The surface starts to densify sooner than the specimen's core, as it gets additional heat by conduction from the hotter, preheated furnace air. This leads to a preferential densification of the surface and creates a dense, airtight surface shell which propagates towards the specimen core as the densification continues [36,37]. This was evidenced by microstructures of fast-fired alumina ceramics that showed the surface dense shell growing into the porous core of the specimen, eventually growing through the whole specimen core, and resulting in more than 99 % dense alumina [36,37].

However, in the case of fast-fired YSZ ceramics, the densification sometimes prematurely stops, leaving a specimen with a characteristic structure – densified surface shell and porous core. Since the first reports by Chen and Mayo in 1990s [28,29], it was believed that once the dense surface shell is formed, it geometrically constrains further densification of the porous core. This has been questioned by Kim and Kim [27], who were able to prevent limited densification by thermal purification of the YSZ green bodies prior to the fast firing. They proposed residual chlorine, a remnant of powder synthesis, being the critical factor during the fast densification of 3 mol% yttria-stabilized zirconia (3YSZ) and 8 mol% yttria-stabilized zirconia (8YSZ). While in conventional sintering, there is plenty of time for residual chlorine to vaporize before the pores are closed, the rapid pore closure and formation of an airtight surface shell during fast firing process causes chlorine entrapment. Later

volatilization of chlorine in closed pores pressurizes the specimen from the inside, effectively stopping densification or even causing de-densification – observed as sample swelling. Kim and Kim's pioneering work was later supported by other authors [30,31], showing that the characteristic shell-like structure can in fact be avoided and relatively large YSZ samples can be fully densified by fast firing in a few minutes. The determining factor of success or failure is the presence of the residual chlorine in the sintered powders.

Although flash sintering creates the opposite thermal gradient to fast firing due to its inside-out heating, it still produces an enormously high heating rate up to 10^4 °C/min which might cause chlorine entrapment, and a recent flash sintering article by Seko et al. [24] showed a familiar shell-like structure, indistinguishable from that we observed during fast firing of the same 8YSZ powder [31]. Seko et al.'s first report of this shell-like structure in flash sintered 8YSZ does not provide a convincing explanation of why the structure has been formed, nor is there a mention of residual chlorine, which we believe plays a critical role in fast densification of YSZ ceramics. As full densification is often a primary target, we aim to clarify how the residual chlorine interacts with the densifying YSZ powder compact during the flash sintering and how the presence of residual chlorine provides a good explanation to the contradictory literature reports, where some of the YSZ powders can fully densify and others cannot.

2. Experimental

2.1 Sample preparation

Five different powder grades of commercially available yttria-stabilized zirconia from Tosoh Corp., Japan, were tested in this study. Three of them were binderless: TZ-3Y, TZ-3Y-E, TZ-8Y, and the other two contained binder: TZ-3YB, TZ-3YB-E (batch numbers are included in Table 1). As-received powders were compacted into bar-shaped green bodies in a steel die at a pressure of ~ 15 MPa and then cold isostatically pressed at 250 MPa in a hydraulic press. All the green bodies were annealed at 600 °C for 2 h (denoted as "standard") and two holes for electrodes were drilled at both ends. In addition to this standard set of green bodies, two other sets were prepared. Some green bodies were additionally thermally treated at 1000 °C for 10 h using a heating rate of 5 °C/min (denoted as

"thermally purified") and some green bodies were submerged in a 28 % aqueous solution of NH_4OH at room temperature for 24 h and then left to dry in a fume hood for 24 h (denoted as "chemically purified"). For all the green bodies, Pt paste was painted inside the drilled holes and around electrodes, creating a gauge section of around 5.4 × 4.1 × 16.5 mm.

2.2 Flash sintering

The flash sintering was carried out in an air atmosphere using a vertical high-temperature furnace. The specimens were suspended by stainless steel wires that also served as the electrodes, connecting a green body to a DC power supply (EA-PSI 9750-60, Elektro-Automatik GmbH & CO. KG, Germany). The control of the power supply and electrical data recording was utilized via LabVIEW software. Once the furnace temperature reached 900 °C, the electric field of 60 V/cm was applied to the specimen. As the flash event started and the power dissipation in the sample gradually increased, the power supply was switched from the voltage control to power control, limiting the maximum power to 60 W. The dwell time in the flash state at 60 W was either 5 s, 30 s, 2 min, or 10 min. Then the power supply was turned off and the furnace slowly cooled down to room temperature.

2.3 Sample characterization

The relative densities of green bodies and flash sintered samples were measured based on the Archimedes principle (EN 623-2) using a theoretical density listed in material data sheets as follows: 6.05 g/cm^3 (TZ-3Y, TZ-3YB, TZ-3Y-E, TZ-3YB-E powders) and 5.99 g/cm^3 (TZ-8Y powder). The densities of flash sintered samples were measured by using the anode part of the densified gauge section as illustrated in Fig. 1. The cathode part of the gauge section was broken into several pieces. The fracture surfaces were subsequently characterized by scanning electron microscopy (SEM, Carl Zeiss Merlin). The SEM images were taken from areas close to the original specimen's surface and from the core. The average grain size was calculated by using the linear intercept method.

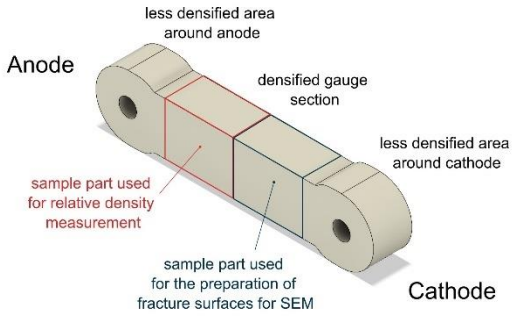

Figure 1 Schematic of the flash sintered sample showing sample part used for density measurements.

The amount of residual chlorine was measured on an X-ray fluorescence (XRF) wave dispersive spectrometer (S8 Tiger, Bruker). The samples were analyzed as loose powders in a helium atmosphere. The QuantExpress software was used for the data evaluation using the Best Detection Limit atmHE method with the detection limit 0.02 wt% of chlorine.

3. Results

3.1 Green body density prior to flash sintering

The relative densities of green bodies are listed in Table 1. The standard green bodies had relative densities between 47.4 and 48.3 %TD, depending on powder grade. As expected, binder-containing "B" grades, which are specifically designed for dry pressing, reached a slightly higher green body density. The additional heat purification at 1000 °C for 10 h led to a slight shrinkage and an increment in relative density. The additional chemical purification in 28 % NH_4OH did not affect green body density.

Table 1 Relative densities of standard, thermally purified, and chemically purified green bodies.

Green body	Powder batch number	Relative density (%TD)		
		Standard	Thermally purified	Chemically purified
TZ-3Y	Z304609P	47.7	49.9	47.7
TZ-3YB	Z300889B	48.3	51.1	-
TZ-3Y-E	Z301043P	47.4	50.9	-
TZ-3YB-E	Z300453B	48.1	51.9	-
TZ-8Y	Z809887P	47.8	49.5	-

3.2 Densification of flash sintered compacts

The electrical characteristics of selected flash sintered samples are shown in the supplementary Fig. S1. The voltage and current exhibited the usual trends (Fig. S1a-b), and power was limited to 60 W for all samples (Fig. S1c). Fig. 2 compares the densification of TZ-3Y and TZ-3YB samples, two powder grades that differ only by the content of the binder. Ultra-fast densification was initially seen in all samples; the relative density rapidly increased in the first few seconds of the flash state. The standard TZ-3Y and TZ-3YB samples reached 84.7 and 87.7 %TD, respectively, after 5 s in the flash state. The densification of binder-containing standard TZ-3YB samples continued to a nearly full density, reaching 99.4 %TD after 10 min in the flash state. The subsequent densification of standard TZ-3Y samples was notably different from TZ-3YB samples; it almost stopped, limiting the final density to around 92 %TD. As is also shown in Fig. 2, the limit to densification seen in standard TZ-3Y samples was removed by both thermal and chemical purification of the green bodies. These purified samples continued to sinter to high densities, in a similar way to standard TZ-3YB samples.

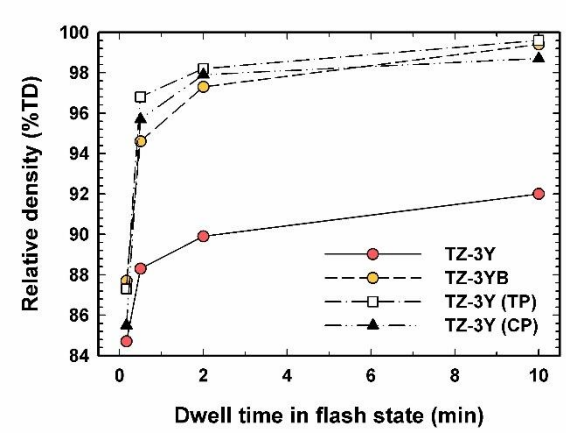

Figure 2 Relative densities of standard TZ-3Y, standard TZ-3YB, thermally purified TZ-3Y (TP), and chemically purified TZ-3Y (CP) samples flash sintered under power control at 60 W for different dwell times.

As for the "E" powder grades, TZ-3Y-E and TZ-3YB-E samples behaved analogously to their non "E" variants (Fig. 3). This means that the standard TZ-3Y-E sample sintered poorly, similarly to the standard TZ-3Y sample, reaching only 92.6 %TD after 10 min in the flash state. The limitation to the final density was again removed by thermal purification prior to flash sintering, allowing a density of

99.8 %TD to be achieved (Fig. 3). The standard TZ-3YB-E sample sintered much better than the standard TZ-3Y-E sample, reaching 99.4 %TD after 10 min in the flash state even without prior purification. This is consistent with the TZ-3YB sample which also did not require purification to achieve a high final density. Clearly, the binder-containing "B" grades are somehow resistant to the limitation of densification. Nevertheless, thermal purification of TZ-3YB-E sample was still beneficial, as it slightly improved the final density from 99.4 to 99.7 %TD.

TZ-8Y powder grade does not have its commercially available "B" counterpart, at least not at the particle size of ~ 60 nm investigated in this study. As shown in Fig. 3, the densification behaviour of TZ-8Y samples was consistent with the other non "B" samples. The standard TZ-8Y sample reached only 87.0 %TD after 10 min in flash state, while thermally purified TZ-8Y sample sintered to 98.7 %TD under the same sintering conditions.

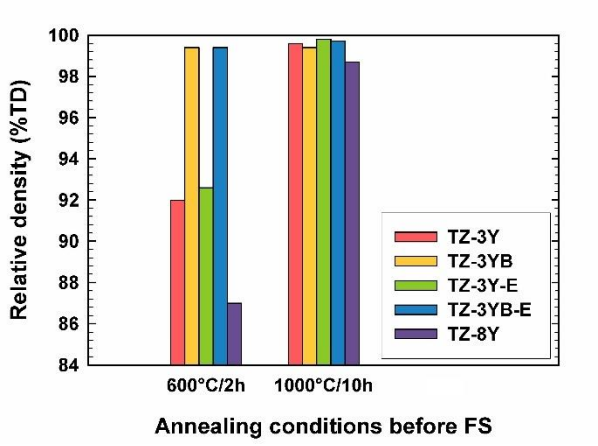

Figure 3 Relative densities of standard (600°C/2h) and thermally purified (1000°C/10h) samples after 10 min in the flash state.

3.3 Microstructure of flash sintered compacts

The microstructures of poorly densified standard TZ-3Y, TZ-3Y-E, and TZ-8Y samples sintered with 10 min dwell time in the flash state were characterised by a shell-like structure as shown in Fig. 4a. The surface densified to almost full density, creating an airtight surface shell (Fig. 4b), while the rest of the sample's volume within the shell remained porous (Fig. 4c, d). No porous core was found in thermally or chemically purified samples (Fig. 4e, f). This is no surprise as these samples attained

almost full density. The binder-containing "B" grade samples (standard TZ-3YB and TZ-3YB-E samples) flash sintered with 10 min dwell time also densified to almost full density with no traces of shell-like structure (Fig. 4g). The grain growth in the porous core under the surface shell (Fig. 4d) was noticeably accelerated compared to the grain growth in samples without shell-like structure (Fig. 4e-g).

3.4 Amount of residual chlorine in sintered powders

The amount of chlorine detected by XRF was the highest in non "B" grade powders: TZ-8Y, TZ-3Y, and TZ-3Y-E powders contained 0.13, 0.09, and 0.08 wt% of chlorine, respectively (Table 2). The "B" grade powders (TZ-3YB and TZ-3YB-E) were either chlorine-free or with a lower than detectable chlorine amount. The XRF analysis confirmed that residual chlorine is lowered by both thermal and chemical purifications. Both approaches diminished the chlorine contamination by approximately two thirds, from 0.09 to 0.03 wt% (Table 2). The presence of ≤ 0.03 wt% of chlorine allowed almost full densification during flash sintering, while chlorine concentrations of ≥ 0.08 wt% resulted in limited densification accompanied by the formation of a shell-like structure.

Table 2 The amount of residual chlorine detected by XRF in loose powders treated under same conditions as green bodies used for flash sintering. The relative densities and average grain size of flash sintered specimens prepared from corresponding powders are also included in the table (flash sintering at 60 W with 10 min dwell time).

Powder grade	Treatment	Chlorine (wt%)	Relative density after sintering (%TD)	Average grain size in the specimen core (μm)
TZ-3Y		0.09	92.0	0.38
TZ-3YB		<DL	99.4	0.25
TZ-3Y-E	600°C/2h + heating up to 900°C	0.08	92.6	0.33
TZ-3YB-E		<DL	99.4	0.23
TZ-8Y		0.13	87.0	1.66
TZ-3Y	600°C/2h + 1000°C/10h + heating up to 900°C	0.03	99.6	0.25
TZ-3Y	600°C/2h + NH_4OH purification + heating up to 900°C	0.03	98.7	0.24

DL stands for detection limit.

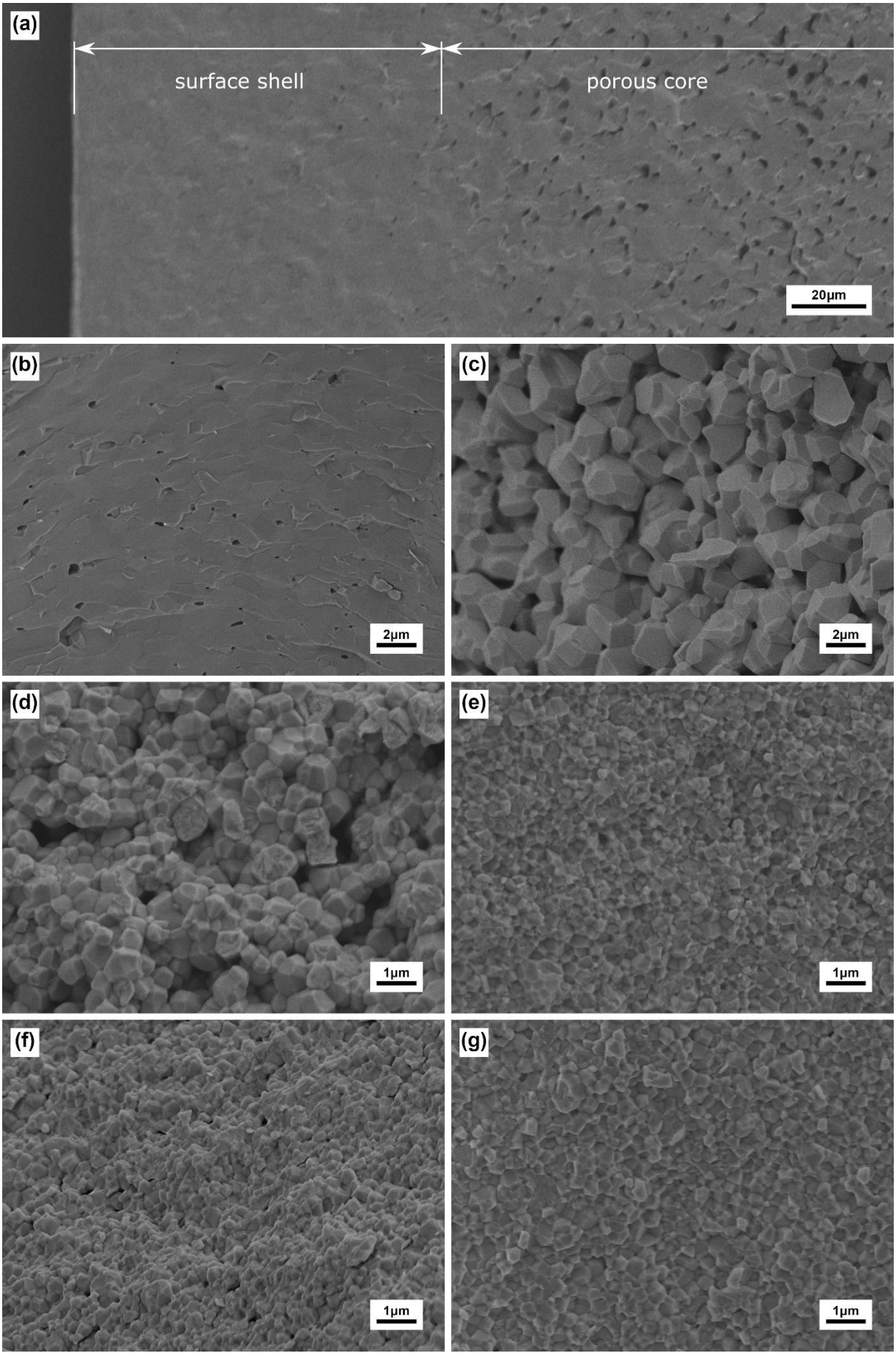
(a)
surface shell
porous core
20μm
(b)
2μm
(c)
2μm
(d)
1μm
(e)
1μm
(f)
1μm
(g)
1μm

Figure 4 Microstructures of samples sintered for 10 min in the flash state. (a) subsurface area of standard, 87.0% dense TZ-8Y sample showing transition between nearly dense surface shell and porous core, (b) porous core of standard, 87.0% dense TZ-8Y sample, (c) nearly dense surface shell of standard, 87.0% dense TZ-8Y sample, (d) porous core of standard, 92.0% dense TZ-3Y sample, (e) nearly dense core of thermally purified, 99.6% dense TZ-3Y sample, (f) nearly dense core of chemically purified, 98.7% dense TZ-3Y sample, and (g) nearly dense core of standard, 99.4% dense TZ-3YB sample. Note the different magnifications of the micrographs, which were required by the different grain sizes.

4. Discussion

Achieving full density during sintering is often one of the main objectives in the ceramic processing. It is a complex task which requires proper choice of powder, shaping technique and sintering method. Many commercially available YSZ powders, including Tosoh TZ-series investigated in this study, are exclusively developed to have an optimal particle size distribution and flowability for easy green body preparation. As for a sintering method, it is important to realize that commercially available powders are mainly designed to be sintered conventionally, i.e., using relatively slow heating rate.

Flash sintering utilizes around 3-4 orders of magnitude higher heating rate compared to conventional sintering and the closed porosity stage is usually reached in a matter of several seconds. Our results in Fig. 2 indicate that the closed porosity stage was indeed reached somewhere between 5 and 30 s in the flash state (by assuming that the transition from interconnected porosity stage to closed porosity stage lies around 92 %TD [38]).

Following the results shown in Fig. 2 and Fig. 3, not all flash sintered compacts achieved high final densities. Binder-containing “B” grade samples (standard TZ-3YB and TZ-3YB-E) densified well and reached more than 99 %TD, while binderless (non “B”) grade samples (standard TZ-3Y, TZ-3Y-E and TZ-8Y) densified poorly. The poor densification was, however, experienced only in the specimens’ core (see Fig. 4), while the surface densified fully in all instances.

It is well-known that full densification can be limited by several phenomena such as entrapment of isolated pores within grains or by entrapment of insoluble gases within the pores [39]. The former is characteristic for ceramics that exhibit high grain boundary mobility. This is not the case of 3YSZ, where the grain growth is usually sluggish, hindered by solute-drag [40]. Although there are cases of "wild" grain growth in flash sintered 3YSZ, causing pore entrapment and abnormal grain growth [17], these require high current densities, much higher than those in this study. Our specimens' temperature in the steady stage of FS under a constant power of 60 W (Fig. S1c) was estimated to be around 1370 °C using the black body radiation model [41]:

$$T = \left(T_0^4 + \frac{W}{A\varepsilon\sigma}\right)^{1/4} \quad (1)$$

where T is the specimen temperature, T_0 is the furnace temperature, W is the power dissipation, A is the surface area of the specimen, ε is the emissivity and σ is Stefan-Boltzmann constant. The emissivity was taken as 0.9, consistent with previous studies [5,11,12,15]. Although the power dissipation during flash sintering was 60 W for all samples, the voltage and current values varied among different samples (Fig. S1a-b). Samples with higher amount of chlorine seemed to exhibit slightly higher electrical conductivity compared to samples with lower amount of chlorine. However, it is hard to determine if this is solely connected to chlorine contamination. It might be also caused by different quality of electrode contacts and/or by different intensity of current localization.

The low final densities of standard TZ-3Y, TZ-3Y-E, and TZ-8Y samples are clearly a consequence of the non-densifying specimen core under the dense surface shell (Fig. 4). Although it may not be obvious from the SEM images, many of these pores are still interconnected. This conclusion is based on the amount of water which was absorbed into the sintered sample during Archimedes density measurements. We propose that the persistence of these pores, and thus, the limited densification is connected to the entrapment of insoluble gases, chloride-based specifically. This comes from the fact that the majority of commercially available YSZ powders are synthesized by hydrolysis of zirconium oxychloride ($ZrOCl_2 \cdot 8H_2O$) and yttrium chloride (YCl_3). Tosoh powders from the TZ-series investigated in this study are no exception to this (Fig. 5).

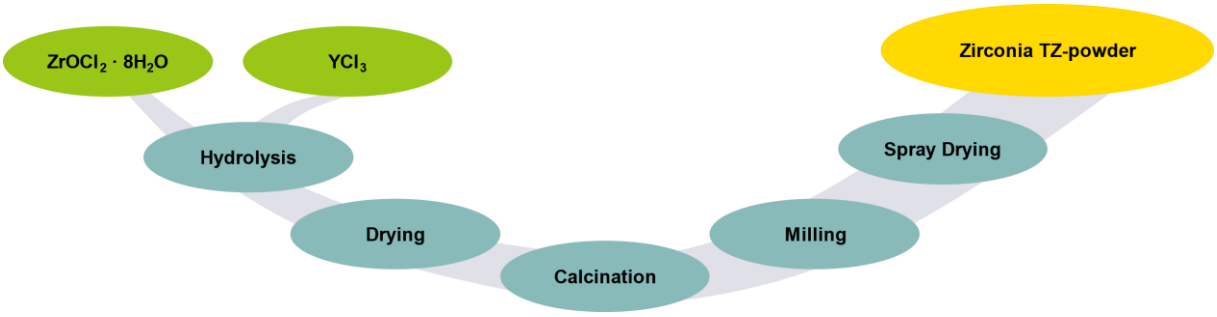

Figure 5 Tosoh zirconia TZ-series manufacturing route adapted from Tosoh Zirconia Brochure [42].

Traces of chlorine have been found in as-received Tosoh TZ-powders several times previously in amounts of 0.07 – 0.20 wt% [27,30,31]. This is because the residual chlorine is strongly adsorbed at the particle surfaces or trapped in the nanopores between individual crystallites [43], making it hard to properly flush out after the hydrolysis step. Although the amount of residual chlorine gradually decreases with increasing calcination/annealing temperature [43], most of the studies on the fast firing of YSZ agreed that thermal treatment at temperatures above 1000 °C is required to reduce the amount of residual chlorine to a level which does not harm the final density [27,30,31]. However, 1000 °C is already high enough to cause nanoparticle growth, and thus, is not commonly used in the YSZ nanopowder manufacturing, allowing the residual chlorine to persist in as-received powders.

The negative effect of entrapped residual chlorine on the densification during rapid sintering is often attributed to an increasing pressure of volatilized chloride species trapped in the shrinking pore network. The chlorine most likely volatilizes as $ZrCl_4$ [30,31], which is insoluble and has a relatively large molecule which limits diffusivity out of the sintered compact. As the dense surface shell prevents $ZrCl_4$ from escaping and more of it is evolving inside the porous core, the sample can eventually increase its dimension (de-densification) which is well-documented phenomenon in fast fired YSZ [27,30,31]. The de-densification can also be seen upon close inspection of recent results on the flash sintering of YSZ. In Yamashita et al.'s [26] study, the relative density firstly increased up to 82.4 %TD during the first minutes of the flash event, but then gradually decreased to 81.2 %TD during 3 h dwell time which is a clear indication of de-densification.

Another effect of residual chlorine is that volatile chloride species significantly promote matter transport via vapor phase. This was the conclusion of Readey and Readey [44] who sintered 3YSZ in a HCl atmosphere. The HCl presumably reacted with ZrO_2, forming $ZrCl_4$ gas, which we expect to be in our samples as well, although not at such a high concentration as in reference [44]. The authors observed almost no densification in their samples, similarly to what we saw in our flash sintered samples after the airtight surface shell developed and the pores inside the sintered specimen were separated from the ambient atmosphere. Readey and Readey explained the lack of densification as a result of an intense particle Ostwald ripening via $ZrCl_4$ vapor; the interparticle necks increased and grains continued to grow but without concurrent densification. The chlorine had the same effect in our samples; the grain size was higher in samples containing a higher amount of residual chlorine (see Table 2).

The entrapment of chlorine obviously becomes more pronounced with increasing heating rate as there is less time for chlorine-based species to escape from the sintered body before the pores are closed. Therefore, the negative effect of residual chlorine on densification is not seen in conventional sintering where the heating rates are typically a few °C/min. This is well evidenced in the study of Saito et al. [45] who sintered chlorine-containing TZ-3Y and TZ-8Y powders in air using a conventional heating rate of 10 °C/min and attained over 99 %TD. The heating rate up to the onset point of the flash sintering is in most cases equivalent to conventional heating rates, however, the onset temperature often lies below 1000 °C, not providing high enough temperature and long enough time for chlorine species to evaporate before the onset of rapid heating.

This is supported by our XRF data shown in Table 2. We measured the amount of residual chlorine at the point where the flash sintering would start, i.e., using powders that were treated in the same way as green bodies, heated up to 900 °C and then cooled down to room temperature. The results support residual chlorine as the cause of poor densification. Binder-containing “B” grade samples (standard TZ-3YB and TZ-3YB-E) densified well because they had no or very little chlorine (< 0.02 wt%), while binderless non “B” grade samples (standard TZ-3Y, TZ-3Y-E and TZ-8Y) densified poorly due to a higher amount of residual chlorine (0.08 – 0.13 wt%).

It is reasonable to assume that a high enough onset temperature would eliminate the rest of the residual chlorine and enabled full densification. This comes from the fact that thermal purification at 1000 °C for 10 h lowered the amount of chlorine from 0.09 to 0.03 wt%. Further evidence for this follows from the results shown in the review Table 3: a higher onset temperature generally resulted in a higher final density. TZ-3Y and TZ-8Y powders, which densified poorly in our study and in many other studies with low onset temperature, were fully densified by Yamashita et al. [10,18] whose onset temperature for flash sintering was 1200 °C – about 300 °C higher than the onset temperature utilized in this study. Residual chlorine also explains well the recent success of shrinkage rate-control flash sintering (SCF) [11–16]. During SCF, the specimen's shrinkage is monitored in real time and the power load is adjusted to maintain the preset shrinkage rate. The power ramp up is relatively slow, producing similar heating rate to conventional sintering. We presume that the success of SCF lies in its similarity to the conventional sintering, i.e. SCF provides enough time for residual chlorine to escape, and thus, allows nearly full densification of TZ-3Y and TZ-8Y compacts seen in several published studies (Table 3, Ref. [11–16]).

Table 3 Review of final densities of flash sintered Tosoh TZ-powders. Only dry pressed, as-received powders are included as additional binder mixing or suspension processing might interact with residual chlorine, and thus, most probably improve the final density.

Tosoh powder grade	Sintering conditions			Final density (%TD)	Linear shrinkage (%)	Reference, first author, publication year
	Advanced regime	T_f (°C)	Current density, power, time in flash state			
Binder-containing "B" grades (TZ-3YB, TZ-3YB-E)						
TZ-3YB	-	850	DC	full	22.5	Cologna et al. (2010) [6]
	-	900	DC, up to 120 mA/mm^2, up to 10 min	99.6	…	Francis et al. (2013) [7]
	-	900	DC, 60 W, 10 min	99.4	…	[This work]
	-	1000	DC, up to 105 mA/mm^2, ~ 12 min	99.6	…	Lebrun et al. (2015) [8]
TZ-3YB-E	-	900	DC, 60 W, 10 min	99.4	…	[This work]
	-	1000	AC (1 kHz), ~ 80 mA/mm^2, 5 min	98.6	…	Carvalho et al. (2018) [9]
Binderless non "B" grades (TZ-3Y, TZ-3Y-E, TZ-8Y)						
TZ-3Y	-	770	AC (100 Hz), 1000 mA (82 mA/mm^2), 5 min	…	18.3	Yamashita (2020) [10]
	-	772	AC (1 kHz), 1200 mA, 5 min	…	19.9	Koike et al. (2022) [15]
	-	780	AC (1 kHz), 800 mA, 5 min	88.8	20.5	Ishino et al. (2021) [11]
	-	820	AC (100 Hz), 1 A, 5 min (also 3 h)	82.5	…	Yamashita et al. (2019) [26]

	-	900	DC, 60 W, 10 min	92.0	…	[This work]
	-	960	AC (10 Hz), 33 mA/mm^2, 60 min	…	21	Kurachi et al. (2020) [22]
	-	1000	AC (100 Hz), 1000 mA (82 mA/mm^2), 5 min	…	20.7	Yamashita (2020) [10]
	-	1100	AC (100 Hz), 1000 mA (82 mA/mm^2), 5 min	…	21.7	Yamashita (2020) [10]
	-	1200	AC (100 Hz), 1000 mA (82 mA/mm^2), 5 min	full	22.5	Yamashita (2020) [10]
	SCF	780	AC (1 kHz), from 50 to 800 mA, 5 min	99.8	22.3	Ishino et al. (2021) [11]
	SCF	781	AC (1 kHz), from 100 to 1200 mA, 5 min	99.9	22.3	Koike et al. (2022) [15]
	SCF	930	AC (1 kHz), from 100 to 1200 mA, 5 min	99.8	22.2	Ishino et al. (2021) [12]
TZ-3Y-E	-	900	DC, 60 W, 10 min	92.6	…	[This work]
	-	995	AC (1 kHz), up to 200 mA/mm^2, 1 min	92.1	…	Lavagnini et al. (2021) [23]
TZ-8Y	-	740	AC (1 kHz), 1200 mA, 5 min	…	17.1	Koike et al. (2022) [15]
	-	800	AC (1 kHz), 60 mA/mm^2, up to ~ 13 min	85	…	Steil et al. (2013) [20]
	-	830	DC, 150 mA/mm^2, few mins	95	…	Bhandari et al. (2022) [25]
	-	870	AC (1 kHz), 1200 mA, 5 min	…	21.1	Taguchi et al. (2021) [13]
	-	870	AC (1 kHz), 1200 mA, 5 min	92	21.1	Taguchi et al. (2021) [14]
	-	900	AC (1 kHz), ~ 40 W, up to 60 min	90	…	Seko et al. (2022) [24]
	-	900	AC (1 kHz), 60 mA/mm^2, up to ~ 13 min	87.8	…	Steil et al. (2013) [20]
	-	900	DC, 60 W, 10 min	87.0	…	[This work]
	-	970	AC (60, 1000 Hz), 8-20 V, few minutes	94	…	Muccillo et al. (2011) [19]
	-	975	AC (1 kHz), 60 mA/mm^2, up to ~ 13 min	94	…	Steil et al. (2013) [20]
	-	1070	AC (50 Hz), 50 V/cm, 1 min	95.7	18	Du et al. (2016) [21]
	-	1200	AC (100 Hz), 1000 mA (82 mA/mm^2), 5 min	97.5	22.5	Yamashita (2020) [18]
	SCF	754	AC (1 kHz), from 100 to 1200 mA, 5 min	98.7	22.3	Koike et al. (2022) [15]
	SCF	870	AC (1 kHz), from 100 to 1200 mA, 5 min	99	22.9	Taguchi et al. (2021) [13]
	SCF	870	AC (1 kHz), from 100 to 1150 mA, 5 min	99.7	23.1	Taguchi et al. (2021) [14]
	SCF	870	AC (1 kHz), from 100 to 1200 mA, 5 min	…	23.5	Koike et al. (2022) [16]

The poor densification of YSZ compacts seems to be always accompanied by the formation of a shell-like structure [24,29–31], where the surface is highly dense while the core is porous. This is understandable in the case of fast firing, where the heat flux comes from the heating elements and hot furnace atmosphere. Preferential densification of a surface creates the dense surface shell and further

densification of the porous core is stopped due to evolution of chlorine-based gases. Although flash sintering exhibits the opposite thermal gradient due to its inside-out heating, the pore closure is even faster than in the case of fast firing, lasting only few seconds. Therefore, we assume that the chlorine species are trapped in all closing pores, but they eventually diffuse away from the near-surface layer, enabling full densification of the surface shell.

As for the different densification behaviour of various commercially available Tosoh TZ-powders, binder-containing "B" grades seem to be immune to poor densification. Both standard TZ-3YB and TZ-3YB-E samples achieved more than 99 %TD after 10 min in the flash state (Fig. 3). This finding is very consistent with other researchers' results as shown in Table 3. According to the manufacturer's material data sheets, the only difference between binderless TZ-3Y grade and binder-containing TZ-3YB grade is in the binder content. The other powder characteristics such as specific surface area and chemical composition are identical. The same can be said comparing TZ-3Y-E and TZ-3YB-E grades, which in addition to non "E" variants contain 0.1-0.4 wt% of alumina.

The TZ-3Y and TZ-3YB powders used in this study were analysed by XRF in our previous work, each having ~ 0.07 wt % of chlorine in the as-received state (Table 2 in Ref. [31]). Traces of chlorine were also found in the other powder grades which shows that residual chlorine is present in all as-received Tosoh TZ-powders. The important consideration is, however, how much chlorine is in the green body at the onset of rapid densification. All the green bodies used in the present study were annealed at least at 600 °C for 2 h and then heated up to 900 °C before the flash sintering onset. Taking results from our previous work [31], chlorine-species volatilized from "B" grade samples during binder burnout at around 400 °C as proved by mass spectroscopy (Figure 5 in Ref. [31]), effectively lowering the amount of residual chlorine by ~ 65 % compared to the as-received state. On the contrary, there were no traces of chlorine-species coming from the non "B" grade green bodies around this temperature. The present study provides a further insight into the kinetics of chlorine removal. At 900 °C, chlorine still persists in TZ-3Y powder in an amount of 0.09 wt% (which is roughly the same quantity as detected in the as-received powder [31]), while in TZ-3YB sample, there were no measurable traces of chlorine, proving that the "B" grade powders are a better choice for flash sintering.

Whether this is due to more intensive heat generation upon binder decomposition in “B” grade powders, due to reactive products of binder decomposition that would engage and remove adsorbed chlorine, or due to other aspects remains unclear and is difficult to evaluate because the exact binder composition and synthesis route of Tosoh TZ-powders are commercially confidential. Nevertheless, the reduction of chlorine content in “B” grades prior to the onset of flash sintering correlates well with the completely different densification behaviour. While standard TZ-3Y, TZ-3Y-E, and TZ-8Y samples reached only around 90 %TD, standard TZ-3YB and TZ-3YB-E samples sintered to more than 99 %TD (Fig. 3).

Thermal purification at or above 1000 °C for several hours has been previously reported as a method of removing residual chlorine from green bodies [27,30,31]. Such treated YSZ samples were successfully sintered by fast firing to almost full density. The same thermal treatment also remarkably improved densification in our flash sintered samples as displayed in Fig. 3. As shown in Table 2, thermal purification reduced the chlorine amount by approximately two thirds, from 0.09 to 0.03 wt%. This low amount was just at the detection limit of XRF and was measured only by the most sensitive Best Detection Limit atmHE method, otherwise no chlorine was detected in purified samples.

Fig. 6 displays the dependence of the final density of various Tosoh TZ-samples on the amount of residual chlorine. Although the data come from studies on fast firing (except data from this work), include various Tosoh TZ-powder grades and sintering conditions, and rely on various analytical techniques with different precision, one can estimate the borderline of critical chlorine concentration. It seems that chlorine concentration ≤ 0.03 wt% is safe and represents a good condition for attaining full density, while chlorine concentrations higher than 0.06 wt% will significantly impair densification during rapid sintering.

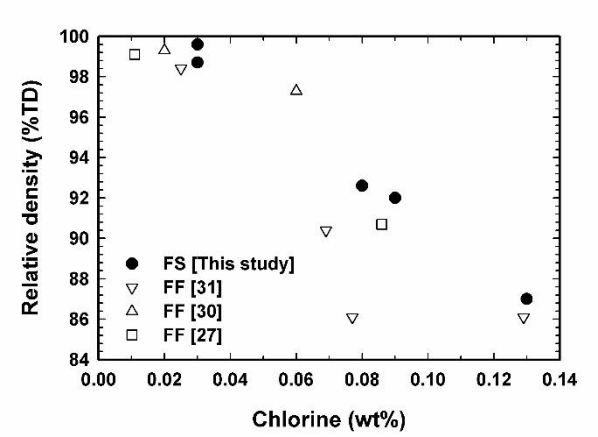

Figure 6 Dependence of the final density of flash sintered (FS) and fast fired (FF) Tosoh TZ-samples on the amount of residual chlorine.

We also performed another route to eliminate residual chlorine – green body purification in 28 % NH_4OH. It is well-known that the purification in NH_4OH is often used during laboratory synthesis of YSZ powders, precisely because of the removal of residual chlorine. As shown in Table 2, the amount of chlorine was reduced to 0.03 wt%, a similar level as after thermal purification. The subsequent flash sintering of a chemically purified green body resulted in a high final density as shown in Fig. 2 and prevented shell-like structure formation. This further supports the residual chlorine as a prime factor behind poor densification of some flash sintered YSZ ceramics.

Conclusions

Densification during flash sintering of yttria-stabilized zirconia ceramics, synthesized from chloride-based precursors, is negatively influenced by residual chlorine. As the densification time into closed porosity stage lasts only several seconds, residual chlorine is trapped inside the pores, and the ongoing volatilization of chlorine-based species acts against further shrinkage. Chlorine near the surface eventually diffuses away, allowing full densification of the surface shell, but the pores in the core become irremovable, effectively stopping densification at around 90 % of theoretical density. To avoid this, chlorine-free YSZ powders should be used preferentially, otherwise a chlorine removal step must be incorporated. The most general approaches of chlorine removal are thermal purification of green bodies at temperature $\geq$ 1000 °C for several hours or chemical purification of green bodies in NH_4OH.

We also show that Tosoh zirconia TZ-powders with added binder, denoted as “B” grades, self-purify of chlorine during binder burnout, and thus, are more optimal choice for flash sintering compared to their non “B” variants.

References

[1] C.E.J. Dancer, Flash sintering of ceramic materials, Mater. Res. Express 3 (2016) 102001.

[2] M. Yu, S. Grasso, R. Mckinnon, T. Saunders, M.J. Reece, Review of flash sintering: materials, mechanisms and modelling, Adv. Appl. Ceram. 116 (2017) 24–60.

[3] M. Biesuz, V.M. Sglavo, Flash sintering of ceramics, J. Eur. Ceram. Soc. 39 (2019) 115–143.

[4] D.- H. Kim, C.H. Kim, Effect of heating rate on pore shrinkage in yttria-doped zirconia, J. Am. Ceram. Soc. 76 (1993) 1877–1878.

[5] W. Ji, J. Zhang, W. Wang, Z. Fu, R. Todd, The microstructural origin of rapid densification in 3YSZ during ultra-fast firing with or without an electric field, J. Eur. Ceram. Soc. 40 (2020) 5829–5836.

[6] M. Cologna, B. Rashkova, R. Raj, Flash sintering of nanograin zirconia in <5 s at 850°C, J. Am. Ceram. Soc. 93 (2010) 3556–3559.

[7] J.S.C. Francis, R. Raj, Influence of the field and the current limit on flash sintering at isothermal furnace temperatures, J. Am. Ceram. Soc. 96 (2013) 2754–2758.

[8] J.M. Lebrun, T.G. Morrissey, J.S.C. Francis, K.C. Seymour, W.M. Kriven, R. Raj, Emergence and Extinction of a New Phase during On-Off Experiments Related to Flash Sintering of 3YSZ, J. Am. Ceram. Soc. 98 (2015) 1493–1497.

[9] S.G.M. Carvalho, E.N.S. Muccillo, R. Muccillo, Electrical behavior and microstructural features of electric field-assisted and conventionally sintered 3 mol % yttria-stabilized zirconia, Ceramics 1 (2018) 3–12.

[10] Y. Yamashita, T. Kurachi, T. Tokunaga, H. Yoshida, T. Yamamoto, Blue photo luminescence from 3 mol%Y_2O_3-doped ZrO_2 polycrystals sintered by flash sintering under an alternating current electric field, J. Eur. Ceram. Soc. 40 (2020) 2072–2076.

[11] Y. Ishino, K. Taguchi, A. Kodaira, T. Tokunaga, T. Yamamoto, Rapid sintering of 3 mol% Y_2O_3-doped ZrO_2 by a combined rapid furnace heating and shrinkage-controlled flash sintering protocol, J. Ceram. Soc. Japan 129 (2021) 551–554.

[12] Y. Ishino, K. Taguchi, M. Koike, T. Tokunaga, T. Yamamoto, Shrinkage rate control during a flash state by current-ramping for 3 mol% Y_2O_3-doped ZrO_2 polycrystals, J. Am. Ceram. Soc. 104 (2021) 4960–4967.

[13] K. Taguchi, Y. Ishino, T. Tokunaga, T. Yamamoto, Constant shrinkage rate control during a flash event for 8 mol% Y_2O_3-doped ZrO_2 polycrystals, J. Ceram. Soc. Japan 129 (2021) 204–207.

[14] K. Taguchi, Y. Ishino, T. Tokunaga, T. Yamamoto, Near complete densification of flash sintered 8YSZ: controlled shrinkage rate effects, J. Eur. Ceram. Soc. 41 (2021) 4567–4571.

[15] M. Koike, A. Kodaira, T. Tokunaga, T. Yamamoto, Shrinkage-rate controlled flash sintering for 3–10 mol% Y_2O_3-doped ZrO_2 polycrystals, J. Ceram. Soc. Japan 130 (2022) 906–912.

[16] M. Koike, Y. Ishino, T. Tokunaga, T. Yamamoto, A first attempt of automated shrinkage-rate control flash sintering using a current profile without feedback of shrinkage behavior for 8 mol% Y_2O_3-doped ZrO_2, J. Ceram. Soc. Japan 130 (2022) 327–330.

[17] V. Prajzler, K. Maca, P. Šťastný, R.I. Todd, Abnormal grain growth in DC flash sintered 3-mol% yttria-stabilized zirconia ceramics, J. Am. Ceram. Soc. 105 (2022) 5562–5568.

[18] Y. Yamashita, A. Itoh, T. Tokunaga, H. Yoshida, T. Yamamoto, Blue photoluminescence at room temperature from Y_2O_3-doped ZrO_2 polycrystals sintered by flash sintering, Appl. Phys. Express 13 (2020) 035506.

[19] R. Muccillo, M. Kleitz, E.N.S. Muccillo, Flash grain welding in yttria stabilized zirconia, J. Eur. Ceram. Soc. 31 (2011) 1517–1521.

[20] M.C. Steil, D. Marinha, Y. Aman, J.R.C. Gomes, M. Kleitz, From conventional ac flash-sintering of YSZ to hyper-flash and double flash, J. Eur. Ceram. Soc. 33 (2013) 2093–2101.

[21] Y. Du, A.J. Stevenson, D. Vernat, M. Diaz, D. Marinha, Estimating Joule heating and ionic conductivity during flash sintering of 8YSZ, J. Eur. Ceram. Soc. 36 (2016) 749–759.

[22] T. Kurachi, Y. Yamashita, T. Tokunaga, H. Yoshida, T. Yamamoto, Suppression of nitridation of yttria-doped zirconia during flash sintering, J. Am. Ceram. Soc. 103 (2020) 3002–3007.

[23] I.R. Lavagnini, J. V. Campos, E.M.J.A. Pallone, Microstructure evaluation of 3YSZ sintered by Two-Step Flash Sintering, Ceram. Int. 47 (2021) 21618–21624.

[24] M. Seko, K. Hattori, Y. Ishino, A. Kodaira, T. Tokunaga, T. Yamamoto, Shell-like structure to limit further densification formed during flash sintering under alternative current electric field for 8 mol% Y_2O_3-doped ZrO_2, J. Ceram. Soc. Japan 130 (2022) 895–898.

[25] S. Bhandari, T.P. Mishra, O. Guillon, D. Yadav, M. Bram, Accessing the role of Joule heating on densification during flash sintering of YSZ, Scr. Mater. 211 (2022) 114508.

[26] Y. Yamashita, T. Kurachi, T. Tokunaga, H. Yoshida, T. Yamamoto, Technique to control specimen electric current during a flash state with alternating current electric fields, J. Ceram. Soc. Japan 127 (2019) 849–851.

[27] D.- H. Kim, C.H. Kim, Entrapped Gas Effect in the Fast Firing of Yttria- Doped Zirconia, J. Am. Ceram. Soc. 75 (1992) 716–718.

[28] D.-J. Chen, M.J. Mayo, Densification and grain growth of ultrafine 3 mol% Y_2O_3-ZrO_2 ceramics, Nanostruct. Mater. 2 (1993) 469–478.

[29] D.-J. Chen, M.J. Mayo, Rapid rate sintering of nanocrystalline ZrO_2-3 mol% Y_2O_3, J. Am. Ceram. Soc. 79 (1996) 906–912.

[30] S.M. Sweeney, M.J. Mayo, Origin of unusual sintering phenomena in compacts of chloride-derived 3Y-TZP nanopowders, Science of Sintering 46 (2014) 169–184.

[31] V. Prajzler, S. Průša, K. Maca, Rapid pressure-less sintering of fine grained zirconia ceramics: Explanation and elimination of a core-shell structure, J. Eur. Ceram. Soc. 39 (2019) 5309–5319.

[32] D. Hotza, D.E. García, R.H.R. Castro, Obtaining highly dense YSZ nanoceramics by pressureless, unassisted sintering, Int. Mater. Rev. 60 (2015) 353–375.

[33] V. Prajzler, D. Salamon, K. Maca, Pressure-less rapid rate sintering of pre-sintered alumina and zirconia ceramics, Ceram. Int. 44 (2018) 10840–10846.

[34] T.S. Possamai, R. Oba, V.P. Nicolau, D. Hotza, D.E. García, Numerical simulation of the fast firing of alumina in a box furnace, J. Am. Ceram. Soc. 95 (2012) 3750–3757.

[35] D. Salamon, R. Kalousek, J. Zlámal, K. Maca, Role of conduction and convection heat transfer during rapid crack-free sintering of bulk ceramic with low thermal conductivity, J. Eur. Ceram. Soc. 36 (2016) 2955–2959.

[36] D.E. García, J. Seidel, R. Janssen, N. Claussen, Fast firing of alumina, J. Eur. Ceram. Soc. 15 (1995) 935–938.

[37] D.E. García, D. Hotza, R. Janssen, Building a sintering front through fast firing, Int. J. Appl. Ceram. Technol. 8 (2011) 1486–1493.

[38] T. Spusta, J. Svoboda, K. Maca, Study of pore closure during pressure-less sintering of advanced oxide ceramics, Acta Mater. 115 (2016) 347–353.

[39] S.J.L. Kang, What we should consider for full densification when sintering, Materials 13 (2020) 3578.

[40] K. Matsui, H. Yoshida, Y. Ikuhara, Grain-boundary structure and microstructure development mechanism in 2-8 mol% yttria-stabilized zirconia polycrystals, Acta Mater. 56 (2008) 1315–1325.

[41] R.I. Todd, E. Zapata-Solvas, R.S. Bonilla, T. Sneddon, P.R. Wilshaw, Electrical characteristics of flash sintering: thermal runaway of Joule heating, J. Eur. Ceram. Soc. 35 (2015) 1865–1877.

[42] Tosoh Zirconia Brochure, Tosoh Corporation, available from: https://www.rbhltd.com/wp-content/uploads/2019/05/Tosoh-Zirconia-Brochure.pdf

[43] M. Valigi, A. Cimino, D. Gazzoli, G. Minelli, The influence of additives (Cl^-, ReO_4^-, Ti(IV)) on some properties of ZrO_2, Solid State Ion. 32–33 (1989) 698–705.

[44] M.J. Readey, D.W. Readey, Sintering of ZrO_2 in HCl Atmospheres, J. Am. Ceram. Soc. 69 (1986) 580–582.

[45] N. Saito, T. Ikegami, Influence of chlorine on sintering of yttria-doped zirconia, J. Ceram. Soc. Japan 109 (2001) 738–741.

Acknowledgement

The research was funded by Czech Science Foundation (GAČR), project No. 22-30487O. The authors also acknowledge use of characterisation facilities within the David Cockayne Centre for Electron Microscopy, Department of Materials, University of Oxford, alongside financial support provided by the Henry Royce Institute (Grant ref EP/R010145/1). The performing of the XRF analysis by Hana Kaňková, PhD. from the FunGlass centre, Trenčín, Slovakia, is gratefully acknowledged.